Accurate measurements of the pitch-angle scattering of beam ions

W. W. Heidbrink
Department of Physics and Astronomy, University of California, Irvine, California 92697

(Received 7 August 2001; accepted 8 October 2001)

The pitch-angle scattering rate of a dilute population of 75 keV deuterium ions is measured in a well-diagnosed, relatively quiet, magnetically-confined deuterium plasma. Neutral particle diagnostics detect the fast-ion density in velocity space following a short 10 ms pulse of injected beam ions. The data are compared to the classical theory of diffusion in velocity space caused by many, small-angle, Coulomb-scattering events. Within uncertainties of $\lesssim$15%, the data confirm the classical theory. © *2002 American Institute of Physics.* [DOI: 10.1063/1.1423622]

I. INTRODUCTION

Coulomb scattering is a fundamental process in plasma physics that causes an initially monoenergetic beam to decelerate and diffuse in velocity space. An enormous number of phenomena depend upon the angular scattering rate in both natural and laboratory plasmas. Important effects include energy transport, particle transport into any loss cones, the amount of current driven by a beam, and the duration of wave–particle interaction.

In standard treatments, small-angle scattering events predominate, so a statistical theory governs the evolution of the distribution function in velocity space.[1] Consider a dilute population of fast ions in a background plasma with Maxwellian electrons and ions. (Self-collisions are assumed negligible.) The speed of the fast ions v is intermediate between the electron and ion thermal speeds, $v_e \gg v \gg v_i$. For this particularly simple case, the evolution of the fast-ion distribution function f is described by the following Fokker–Planck equation:[2]

$$\begin{aligned}
\frac{\partial f}{\partial t}(v,\zeta,t) = S(v,\zeta,t) & \quad \text{(fast-ion source)} \\
+ \frac{1}{\tau_{se}}\frac{\partial}{\partial v}[(v^3+v_c^3)f] & \quad \text{(electron and ion friction)} \\
+ \frac{1}{2\tau_{se}}\frac{\partial}{\partial v}\left[\frac{v_e^2 m_e}{m_f}+\frac{v_c v_i^2 m_i}{v^3 m_f}\right]\frac{\partial f}{\partial v} & \quad \text{(energy diffusion)} \\
+ \frac{1}{2\tau_{se}}\frac{m_i}{m_f}\frac{Z_{\text{eff}}}{[Z]}\frac{v_c^3}{v^3}\frac{\partial}{\partial \zeta}\left[(1-\zeta^2)\frac{\partial f}{\partial \zeta}\right] & \quad \text{(pitch-angle scattering)} \\
- \frac{eE_\parallel}{m_f}\left[\zeta\frac{\partial f}{\partial v}+\frac{(1-\zeta^2)}{v}\frac{\partial f}{\partial \zeta}\right] & \quad \text{(electric field)} \\
- f/\tau_{cx} & \quad \text{(charge exchange).}
\end{aligned} \tag{1}$$

Here $\zeta = v_\parallel / v$ is the component of the velocity vector that is parallel to the magnetic field, v_c is the critical speed where the friction on the electrons and background ions is equal, and τ_{se} is the slowing-down time on electrons. Figure 1 illustrates the evolution of the fast-ion distribution function as predicted by Eq. (1). For simplicity, the source of fast ions is a delta-function in (v,ζ,t) and electric-field and charge-exchange terms are neglected. As time evolves, the centroid of the distribution moves to lower energies due to electron and ion drag (friction), the contours spread horizontally (in energy) due to energy diffusion, and the contours spread vertically (in ζ) due to pitch-angle scattering.

Theoretically, there are several possible reasons the standard treatment might fail. The theory is predicated on the assumption that multiple small angle collisions predominate. In dense plasmas, subdominant terms are no longer negligible;[3] also, nuclear large-energy transfer events[4] or ''knock-on'' collisions[5–7] can be important, particularly in sparsely populated portions of the distribution function. More fundamentally, the standard theory uses an ad hoc cutoff at small angles to represent the effect of Debye shielding. Reference 8 argues that the correct application of shielding theory alters the scattering coefficients by a factor of 2. Even if the treatment in velocity space is correct, in practical situations in inhomogeneous plasma, the predictions could fail if particle orbits or spatial transport are treated incorrectly.

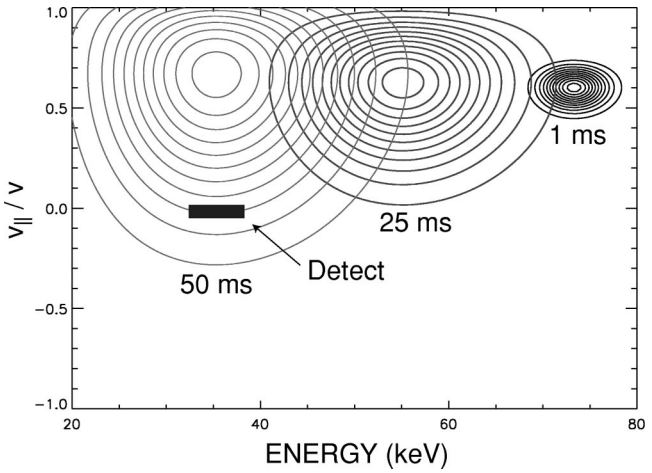

FIG. 1. Linear contours of fast-ion density at three different times as a function of energy and $\zeta = v_{\|}/v$. A monoenergetic source injects 75 keV ions with $\zeta = 0.6$ at $t = 0$. The evolution of the distribution function is calculated by the local analytical solution to the Fokker–Planck equation (Ref. 21) described in the text. The darkened rectangular box represents the velocity-space volume interrogated by the charge-exchange diagnostic.

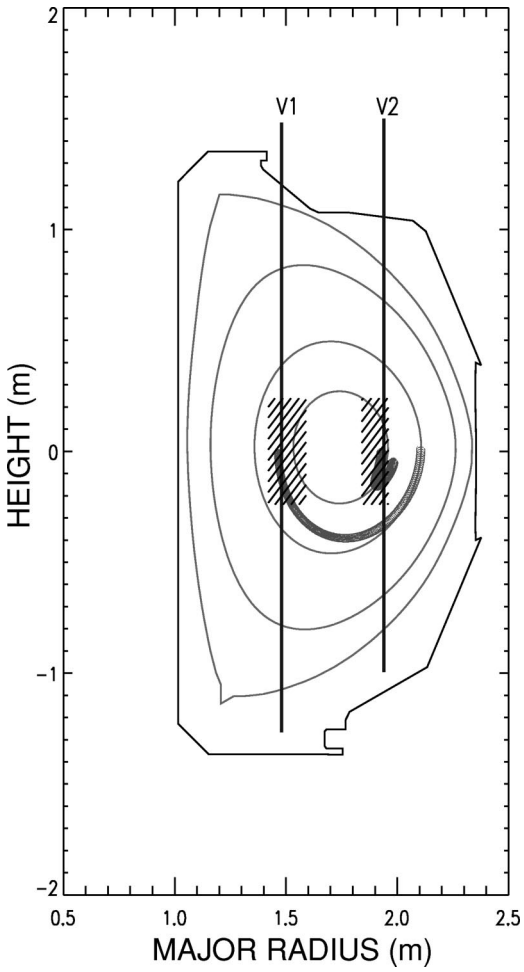

FIG. 2. Elevation of the DIII-D vessel showing the plasma shape for a typical discharge in this study (#93426), the sightlines of the V1 and V2 vertical neutral-particle analyzers, the spatial region of the active charge exchange measurements (hatched), and a typical orbit detected by each of the neutral particle analyzers.

Experimentally, the deceleration of test populations of fast ions is properly described by classical Fokker–Planck theory to within ~10% in tokamak plasmas[9–12] and shows the expected functional dependence on v in a Q-machine.[13] Less is known about velocity-space diffusion, however. In quiet Q-machine plasmas, the parallel velocity diffusion coefficient has the expected dependence on density and velocity.[14] The relaxation rate of an anisotropic distribution is in good agreement with classical theory in pure electron[15] and ion[16] plasmas. In hotter plasmas, wave-induced anisotropies in the electron distribution are modeled using classical theory.[17] The pitch-angle scattering rate in mirror machines can be the same order of magnitude as classical predictions.[18] In tokamaks, the parallel diffusion of beam ions above the injection energy is consistent with classical theory within uncertainties estimated at ~20%.[9] There have also been numerous fast-ion measurements that depend on the pitch-angle scattering rate and appear consistent with classical theory[9,19,20] but the uncertainties, which appear to be of order unity, have not been quantified.

Analysis of escaping neutrals is a standard diagnostic technique in magnetic fusion research. Dozens of papers have compared the charge exchange spectrum during neutral beam injection with simulations; several of these resolved several different pitch angles simultaneously.[9] Two difficulties have prevented accurate quantitative tests of classical theory with these data. First, many early investigations of pitch-angle scattering were hampered by poor knowledge of the background plasma parameters. For example, in 1976 Goldston performed a beautiful experiment with excellent resolution of the fast-ion distribution function in v, ζ, and t but the results could not be compared quantitatively with theory because the effective charge of the plasma Z_{eff} was not known.[21] A second limitation in most of the studies is that they employ ''passive'' charge-exchange measurements that are not spatially resolved, so the measured neutrals originate from regions of the plasma with widely differing pitch-angle scattering rates. A third difficulty in the largest tokamaks is that the line density $n_e l$ is sufficiently high that the reionization probability of escaping neutrals is prohibitively large. The objective of this study is to reproduce Goldston's classic work in a tokamak with (i) excellent background plasma diagnostics, (ii) ''active'' (spatially resolved) charge exchange diagnostics and (iii) modest line density. It is also desirable to operate in a regime where charge-exchange, electric-field, and orbit effects in Eq. (1) are minimized.

With injection of short, 10-ms duration, beam ''blips'' into Ohmically heated plasmas in the DIII-D tokamak, these conditions are realized (Sec. II). Predictions based on classical Fokker–Planck theory (Sec. III) are in good agreement with the measured beam-ion densities (Sec. IV). The estimated uncertainty in the comparison is dominated by uncertainty in Z_{eff} and is estimated as $\sim \pm 15\%$.

II. EXPERIMENTAL TECHNIQUE

The measurements are from DIII-D,[22] a moderately-sized tokamak (major radius $R_0 \simeq 1.7$ m, minor radius

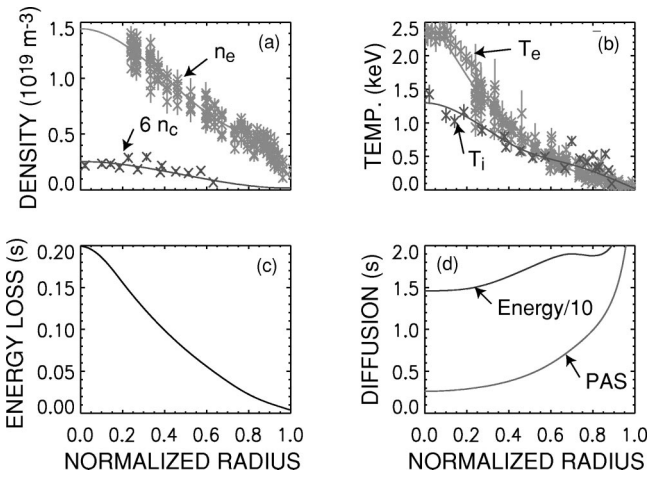

FIG. 3. Profiles of (a) electron and carbon density (multiplied by six), (b) electron and ion temperature, and (c) classical deceleration time $1/\nu_E$, (d) pitch-angle scattering time $1/\nu_\perp$ and energy diffusion time $1/\nu_\parallel$ (divided by ten) in discharge #93426 at 4205 ms. The Coulomb scattering times (Ref. 37) are for 75 keV deuterium ions.

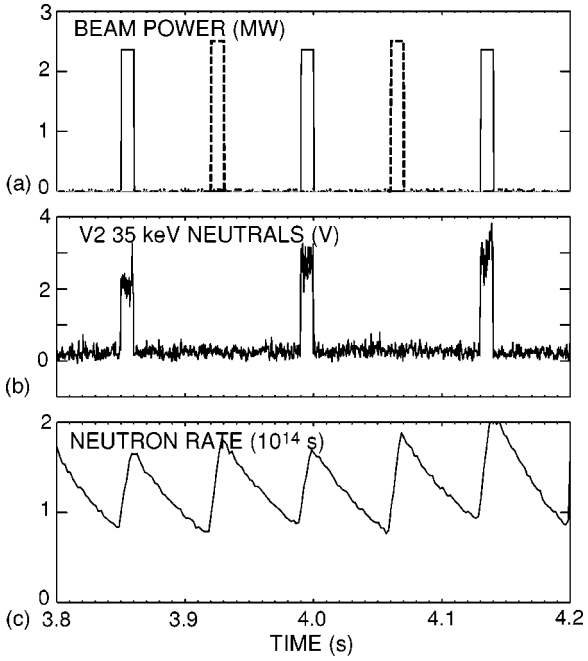

FIG. 4. (a) Injected beam power from the 210° left (solid) and 150° right (dashed) neutral beam sources, (b) V2 signal of 35 keV neutrals, and (c) 2.5 MeV neutron rate as a function of time in discharge #93426.

$a \approx 0.6$ m) operated in the double-null divertor configuration for these experiments. The plasma shape (Fig. 2) is computed by the EFIT code[23] from motional Stark effect (MSE) (Ref. 24) and magnetic probe data. The plasma current is $I_p = 0.6$ MA and the toroidal field is $B_T = 1.9$ T for most of the discharges.

Typical plasma profiles are shown in Fig. 3. The electron density is measured by Thomson scattering[25] corroborated by interferometry.[26] Thomson scattering and electron cyclotron emission[27] measure the electron temperature. The absolutely calibrated charge-exchange recombination (CER) diagnostic[28] measures the ion temperature and bulk plasma rotation. The dominant impurity, carbon from the graphite walls, is also measured by CER.[29] Spectroscopic measurements of low charge states confirm that the carbon density is an order of magnitude larger than the oxygen and helium densities.

The neutral beams inject 71–80 keV deuterium ions in the direction of the plasma current into deuterium plasmas at two angles with respect to the toroidal field. For neutrals injected by the more perpendicular "right" beams the tangency radius is $R_{\tan} \simeq 0.76$ m; for the more tangential "left" beams, $R_{\tan} \simeq 1.15$ m. Approximately 78% of the injected neutrals have the full energy of ~75 keV, while 15% and 7% carry the half and third energies, respectively. In this experiment, the neutral beam sources are typically injected for 10 ms every 70 ms (Fig. 4). TRANSP (Ref. 30) calculations indicate that only about half of the injected beam power is absorbed by the plasma, with the remainder lost to beam shine through (30%–45%), orbit losses to the limiter (~5%), and charge-exchange losses (~5%). The average absorbed beam power of 0.2 MW is somewhat smaller than the Ohmic heating power of ~0.3 MW. Because the confinement and beam thermalization times are longer than 70 ms, the modulation of the beam power has little effect on the background plasma parameters, and the temperature and density profiles in a given discharge are unaffected within experimental uncertainties. The measurements are acquired during the steady-state portion of the discharge when the current is fully diffused. Magnetohydrodynamic (MHD) activity is minimal; there are no detectable coherent magnetic signals and the sawteeth are regular (every ~17 ms) and small (central $\Delta T_e/T_e \simeq 10\%$). The beam-ion density is $\lesssim$4% of the electron density.

The average behavior of the injected beam ions is diagnosed with neutron scintillators.[31] Under these conditions, beam-plasma reactions are calculated to constitute over 95% of the total neutron rate. Since the slowing down time of the beam ions is long compared to the beam pulse duration, the neutron rate rises nearly linearly during each 10 ms beam pulse (Fig. 4). The jump in neutron rate during the beam pulse provides an independent check on the deuterium density.[32] Following the pulse, the neutron rate decays approximately exponentially as the injected beam ions thermalize. Effectively, this volume-integrated measurement constitutes a cross section weighted average of the entire beam population,[33] so the decay of the neutron signal measures the average deceleration of beam ions.[32]

Neutral particle diagnostics[34] measure local densities in phase space. In addition to providing beam ions, some of the beam sources supply neutrals for active charge exchange measurements. The sightline of the V2 neutral particle analyzer intersects neutrals injected by the 210° left source in the hatched spatial region illustrated in Fig. 2; similarly, the V1 sight-line intersects neutrals injected by the 210° right source in the illustrated region. As shown in Fig. 4, the V2 signal is large when the 210° left source provides neutrals for active charge exchange measurements but is barely perturbed when a distant source injects into the plasma. The difference in signal between the local and distant sources is propor-

tional to the emission from the hatched region. The measured signal S is related to the beam-ion distribution function $f(E,\zeta,\mathbf{r})$ by

$$S \propto G \int n_0(\mathbf{r}) \langle \sigma v \rangle_{cx} e^{-\lambda} f(E,\zeta,\mathbf{r}) dl, \tag{2}$$

where G is the gain of the Channeltron detector, n_0 is the neutral density, $\langle \sigma v \rangle_{cx}$ is the charge exchange reactivity, and $e^{-\lambda}$ is the attenuation of escaping neutrals caused by reionization. To relate the measured signal to the average beam-ion density in the volume that produces the active charge exchange signal, $\langle \sigma v \rangle_{cx}$ is computed from the measured energy and n_0 and $e^{-\lambda}$ are calculated using the measured profiles (Fig. 3) in a beam-attenuation code,[29]

$$\overline{f} \propto S/(G n_0 \langle \sigma v \rangle_{cx} e^{-\lambda}). \tag{3}$$

For the data in our experiment the measured energy varies only slightly (from 31 to 35 keV) and the line density $n_e l$ is low, so the denominator of Eq. (3) only varies ~25% for our dataset; the differences between different conditions are readily apparent in the raw signals S.

The experiment is optimized to study velocity space transport. The loop voltage in this steady-state portion of the discharge is only ~0.5 V, so the parallel electric field term in Eq. (1) is negligible. In similar experiments on the Tokamak Fusion Test Reactor (TFTR), the measured spatial diffusion of the beam ions was very small, comparable to the expected neoclassical transport level.[35,36] Although some transport caused by neutralization and subsequent reionization does occur, the global charge exchange losses are small (~5%), so the charge-exchange term in Eq. (1) is relatively unimportant. Similarly, although not ignorable, orbit effects are also relatively unimportant. Figure 2 shows orbits of typical 35 keV beam ions that are detected as active neutrals. For the V2 sightline, the excursion of the orbit from the flux surface is comparable to the spatial resolution of the active charge exchange measurement, $\Delta R/a \lesssim 20\%$. For the V1 chord, the orbit excursion is larger, the spatial resolution is poorer, the uncertainties in beam deposition are greater, and the background correction associated with the passive charge exchange signal is larger, so the data are less reliable as a measure of the local beam-ion distribution function.

III. THEORETICAL MODELING

The measurements are compared with two different calculations of the expected evolution of the beam-ion distribution function. One approach uses an expansion in terms of Legendre polynomials to solve the Fokker–Planck equation [Eq. (1)] for a delta-function source of beam ions.[21] The charge-exchange and electric-field terms are ignored. The coefficients for the friction, energy-diffusion, and pitch-angle scattering terms are evaluated using the fitted plasma profiles (Fig. 3) for each discharge evaluated locally at the radius of the active charge exchange measurement. The solution is computed numerically using the Interactive Display Language (IDL); the computer code was tested by comparing the initial deceleration, energy-diffusion, and pitch-angle scattering of a delta-function source to the rates in the Naval Research Laboratory (NRL) Plasma Formulary.[37] In practice, each 10 ms beam pulse is modeled as the sum of several delta-function sources. The magnitude of the predicted signal is proportional to the local beam-ion deposition computed by the neutral attenuation code.[29]

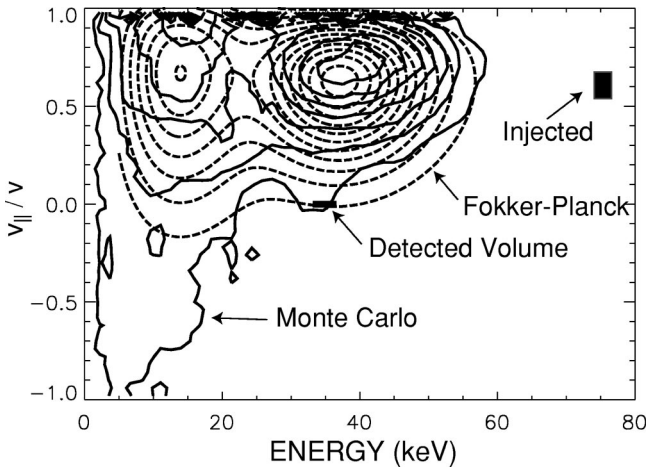

FIG. 5. Comparison of the beam-ion distribution function calculated by the local Fokker–Planck theory (dashed) and the TRANSP Monte Carlo code (solid) for a case where left beams injected 70 and 140 ms prior to an active charge exchange measurement at 35 keV. Discharge #93431.

The second approach uses Monte Carlo modeling as implemented in the TRANSP code.[30] TRANSP follows 10 000 weighted beam particles and includes drift-orbit averaging, charge-exchange, reionization of halo neutrals, rotation and electric field effects, and spatial diffusion associated with neoclassical transport. The full fitted profiles (Fig. 3) are employed in the calculations. TRANSP calculates the distribution function in the entire plasma but, for the comparison with the measurement, f is averaged over the poloidal and radial slice shown in Fig. 2. To reduce the importance of Monte Carlo noise, the computed distribution function is smoothed in energy and ζ.

The calculations are compared in Fig. 5 for a typical case in which two prior beam pulses contribute to the measured signal. On the local Fokker–Planck contours, the pulse that was injected 140 ms earlier appears as a peak at ~14 keV, while the pulse that was injected 70 ms earlier appears as a peak at ~37 keV. Comparison of the two calculations shows that the TRANSP Monte Carlo calculation is both noisier and broader than the analytical Fokker–Planck solution. The statistical fluctuations are an unavoidable feature of the Monte Carlo technique. The broader distribution is associated with the retention of charge exchange, orbit effects, and spatial averaging. The Monte Carlo solution is more accurate but is too computationally expensive to be applied to all of the data.

IV. RESULTS

The available data consist of 188 active charge exchange measurements that follow a short beam blip in a nominally steady-state plasma. Of these, 47 V1 measurements and 34 V2 measurements have all the data needed for a complete comparison with analytical Fokker–Planck theory. For the

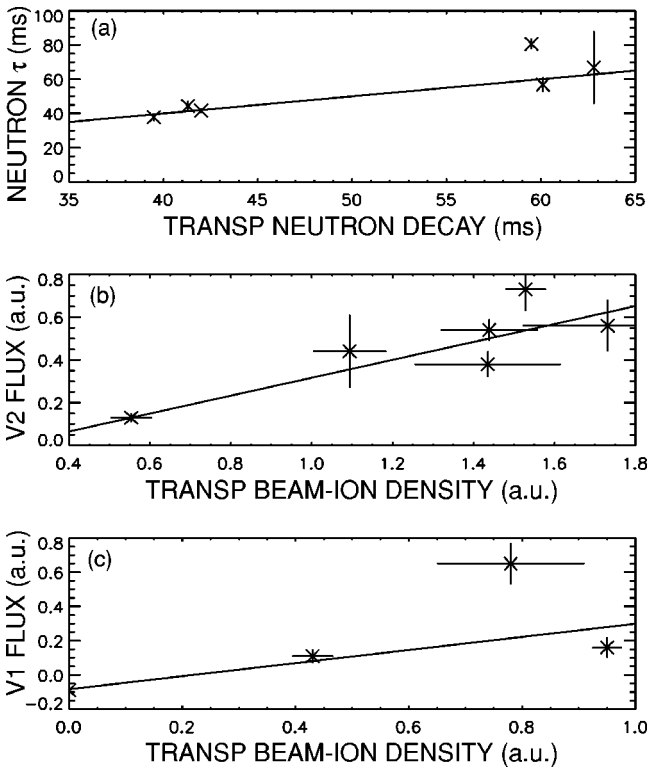

FIG. 6. (a) Measured exponential decay time of the neutron signal vs the calculated exponential decay time for the six discharges in the TRANSP/V2 comparison. (b) Active charge exchange signal from the V2 detector (including corrections for detector gain, neutral reionization, and neutral density) vs the calculated beam-ion density in the same phase space volume. (c) Active charge exchange signal from the V1 detector vs calculated beam-ion density.

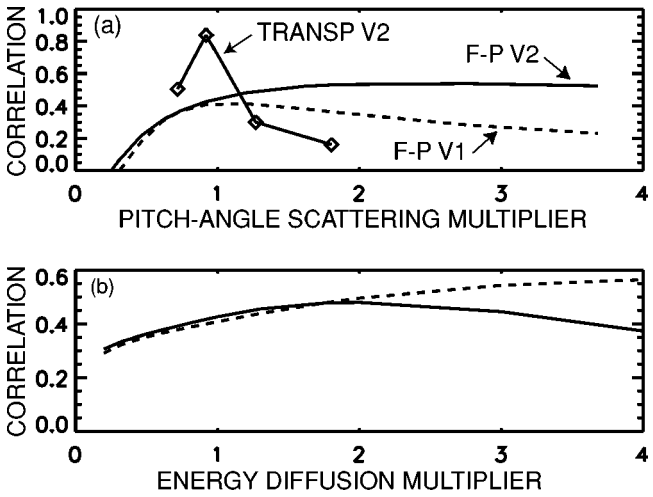

FIG. 7. Correlation coefficient r between experiment and theory as a function of (a) pitch-angle scattering rate multiplier p and (b) energy diffusion multiplier e. The solid line represents comparisons between the local Fokker–Planck theory and the full set of V2 measurements, the dashed line represents comparisons between the local Fokker–Planck theory and the full set of V1 measurements, and the diamonds represent comparisons between the subset of V2 measurements and the TRANSP Monte Carlo calculations. [For example, the diamond at $p=0.93$, $r=0.87$ represents the comparison shown in Fig. 6(b).]

Monte Carlo calculations, ten discharges from the same experimental sequence (shots #93426–93435) with high quality profile data are chosen for detailed analysis.

The results of the comparison with the TRANSP Monte Carlo calculations appear in Fig. 6. An initial check on the quality of the data is to test that the average deceleration rate agrees with classical Coulomb theory, since this dependence has been verified in numerous previous experiments.[9] Figure 6(a) compares the measured exponential decay time obtained from fits to the neutron signal following a beam blip to the exponential decay time calculated by TRANSP. (The same least-squares fitting procedure is used for both ''signals.'') The agreement is satisfactory (correlation coefficient $r=0.87$).

Figure 6(b) compares the measured V2 beam-ion density to the phase-space density calculated by TRANSP. The variation in beam-ion density is primarily due to variation in beam injection angle and beam timing. The agreement between theory and experiment is good ($r=0.84$). If, for example, the computed beam-ion density from a different (incorrect) spatial zone is employed, the agreement is much poorer. Figure 6(c) shows a similar comparison for the V1 measurements. Once again, the agreement is satisfactory ($r=0.65$) but, in this case, fewer measurements are available from the best sequence of discharges.

Although Fig. 6 shows that the classical theory is consistent with the measurements, it does not answer the question, ''Does the classical theory agree better than alternative formulations?'' To address the sensitivity of the results, we artificially multiply the pitch-angle scattering rate by a ''fudge factor'' p and repeat the calculations. The correlation coefficient r is a useful measure of the degree of consistency between experiment and the altered theory. In Fig. 7(a), r is plotted vs the pitch-angle scattering multiplier p for three sets of comparisons: local Fokker–Planck theory with the 34 V2 measurements, local Fokker–Planck theory with the 47 V1 measurements, and TRANSP Monte Carlo calculations with the 6 V2 measurements. (The TRANSP comparison with the V1 data is not shown because the results are insensitive to the pitch angle scattering rate, i.e., $r=0.7-0.8$ for all calculated rates.) In the local Fokker–Planck theory, it is also straightforward to test the sensitivity of the results to the assumed energy-diffusion rate. The results of this comparison are shown in Fig. 7(b).

Figure 7 shows that the classical theory as implemented in the TRANSP calculations provides the best fit to the measurements. For the comparison with TRANSP, the largest correlation coefficient is for a multiplier $p\simeq 1$. The fit is much poorer for either a weaker scattering rate ($p\simeq 0.7$) or for a stronger scattering rate ($p\simeq 1.3$). A similar result is obtained for the comparison between the V1 measurements and the local Fokker–Planck theory. In contrast, for the comparison between the V2 measurement and the local Fokker–Planck theory, the agreement improves if the pitch-angle scattering rate is enhanced over classical theory. A similar result is found for the energy diffusion rate. Referring back to Fig. 5, by neglecting spatial averaging, orbit effects, and charge exchange, the local Fokker–Planck theory underestimates the actual spread of the distribution function. Artificial enhancement of the diffusion rates compensates for this deficiency, improving the agreement with experiment.

To quantify the result, estimates of the random experimental and theoretical uncertainties are required. The experimental uncertainties are readily quantified by forming an ensemble of measurements under nominally identical conditions and calculating the standard deviation. For a given theoretical model, the theoretical uncertainties stem from uncertainties in the measured plasma parameters, especially errors in electron and carbon density. Because the TRANSP calculations are computationally expensive, the sensitivity to these errors are difficult to quantify rigorously. To obtain an estimate, two new sets of TRANSP calculations are performed using modified n_e and n_C profiles and the uncertainty in calculated beam density is obtained by adding the variations in quadrature. The estimated uncertainties are shown in Fig. 6. Armed with these uncertainties, we calculate reduced chi-squared $\tilde{\chi}^2$ for the V2-TRANSP comparison. For the classical pitch-angle theory ($p \simeq 1$), $\tilde{\chi}=1.0$, so the measurements are consistent with the theory. On the other hand, for $p \simeq 0.7$ or $p \simeq 1.3$, $\tilde{\chi}^2=6.9$ and $\hat{\chi}=6.6$, respectively, so there is essentially 0% probability that the modified theory correctly describes the experiment.

There are also possible systematic errors. The energy calibration of the neutral particle analyzer[38] could be erroneous by ~10%. For the measurement of the carbon density, the primary systematic uncertainty is in the charge-exchange excitation rates. Other possible systematic errors, such as the light intensity calibration or changes in transmission efficiency caused by coating of the vacuum windows, are thought to be much smaller, so the overall systematic uncertainty is estimated as ~15%.[29] The electron density is independently measured by two absolutely-calibrated diagnostics, so large systematic uncertainties are unlikely. Another check is the jump in neutron rate during the 10 ms beam pulse. This measurement depends on the deuterium density, which is inferred from the independent electron and impurity measurements. The measured jump agrees with the expected jump within the 15% uncertainty in the absolute calibration of the neutron detector.[31] Overall, the systematic uncertainty appears comparable to the random uncertainty.

V. CONCLUSION

Dilute populations of beam ions in quiet tokamak plasmas are studied. Active charge exchange measurements of ~35 keV ions that have scattered $\Delta v_\parallel / v = 0.4-0.6$ are in good agreement with the predictions of classical Coulomb scattering theory. The uncertainty in the determination of the pitch-angle scattering rate is comparable to the uncertainty in $Z_{\rm eff}$, which is approximately 15%.

The modifications to the standard formulas for Debye shielding proposed in Ref. 8 are incompatible with the data. Although the results show that small-angle scattering predominates in the 10–100 keV range, the study does not address the importance of large-angle scattering events at MeV energies.[7] On the other hand, the agreement between theory and experiment strongly suggests that beam deposition and orbital effects are properly treated by the TRANSP code in this regime. In the core of quiet tokamak plasmas, the deceleration,[32] pitch-angle scattering, and spatial diffusion[35] of beam ions are adequately described by the effects of Coulomb scattering.

ACKNOWLEDGMENTS

The assistance of D. Baker, K. Burrell, E. Carolipio, R. Ellis, M. Miah, M. Wade, P. West, and the entire DIII-D team is gratefully acknowledged.

This work was funded by General Atomics Subcontract No. SC-G903402 under the U.S. Department of Energy Contract No. DE-AC03-99ER54463.

[1] S. Chandrasekhar, Rev. Mod. Phys. **15**, 1 (1943).
[2] D. L. Jassby, Nucl. Fusion **17**, 309 (1977).
[3] C.-K. Li and R. D. Petrasso, Phys. Rev. Lett. **70**, 3059 (1993).
[4] P. Helander, M. Lisak, and D. D. Ryutov, Plasma Phys. Controlled Fusion **35**, 363 (1993), and references therein.
[5] R. K. Fisher, P. B. Parks, J. M. McChesney, and M. N. Rosenbluth, Nucl. Fusion **34**, 1291 (1994).
[6] J. Kallne, L. Ballabio, J. Frenje, S. Conroy, G. Ericsson, M. Tardocchi, E. Traneus, and G. Gorini, Phys. Rev. Lett. **85**, 1246 (2000).
[7] A. A. Korotkov, A. Gondhalekar, and R. J. Akers, Phys. Plasmas **7**, 957 (2000).
[8] D. Li, Nucl. Fusion **41**, 631 (2001).
[9] W. W. Heidbrink and G. J. Sadler, Nucl. Fusion **34**, 535 (1994), and references therein.
[10] K. Tobita, K. Tani, T. Nishitani, K. Nagashima, and Y. Kusama, Nucl. Fusion **34**, 1097 (1994).
[11] ITER Physics Expert Group on Energetic Particles, Heating, and Current Drive *et al.*, Nucl. Fusion **39**, 2471 (1999), and references therein.
[12] F. V. Tchernychev, Y. Kusama, M. Nemoto, A. Morioka, K. Tobita, and S. Ishida, Plasma Phys. Controlled Fusion **41**, 1291 (1999).
[13] D. Newsham, T. J. Ross, and N. Rynn, Phys. Plasmas **3**, 2824 (1996).
[14] J. Bowles, R. McWilliams, and N. Rynn, Phys. Plasmas **1**, 3814 (1994).
[15] B. R. Beck, J. Fajans, and J. H. Malmberg, Phys. Plasmas **3**, 1250 (1996), and references therein.
[16] F. Anderegg, X.-P. Huang, E. M. Hollmann, C. F. Driscoll, T. M. O'Neil, and D. H. E. Dubin, Phys. Plasmas **4**, 1552 (1997).
[17] G. Giruzzi, J. L. Ségui, T. Dudok de Wit, Y. Michelot, Y. Peysson, D. Moreau, and M. Talyard, Phys. Rev. Lett. **74**, 550 (1995).
[18] J. R. Hiskes and A. H. Futch, Nucl. Fusion **14**, 116 (1974), and references therein.
[19] V. A. Yavorskij, J. W. Edenstrasser, V. Y. Goloborod'ko, S. N. Reznik, and S. J. Zweben, Nucl. Fusion **38**, 1565 (1998).
[20] D. Testa and A. Gondhalekar, Nucl. Fusion **40**, 975 (2000).
[21] R. J. Goldston, Nucl. Fusion **15**, 651 (1975).
[22] J. L. Luxon and L. G. Davis, Fusion Technol. **8**, 441 (1985).
[23] L. L. Lao, H. St. John, R. D. Stambaugh, A. G. Kellman, and W. P. Pfeiffer, Nucl. Fusion **25**, 1611 (1985).
[24] B. W. Rice, K. H. Burrell, L. L. Lao, and D. G. Nilson, Rev. Sci. Instrum. **70**, 815 (1999).
[25] T. N. Carlstrom, G. L. Campbell, J. C. Deboo *et al.*, Rev. Sci. Instrum. **63**, 4901 (1992).
[26] T. N. Carlstrom, D. R. Ahlgren, and J. Crosbie, Rev. Sci. Instrum. **59**, 1063 (1998).
[27] Z. Wang, J. Lohr, G. L. Bell, C. Hsieh, J. Luo, R. E. Stockdale, J. B. Wilgen, and J. Zhang, in *Proceedings of the Ninth Joint Workshop on Electron Cyclotron Emission and Electron Cyclotron Heating*, Borrego Springs, 1986, edited by J. Lohr (World Scientific, Singapore, 1995), p. 427.
[28] P. Gohil, K. H. Burrell, R. J. Groebner, and R. P. Seraydarian, Rev. Sci. Instrum. **61**, 2949 (1990).
[29] D. G. Whyte, M. R. Wade, D. F. Finkenthal, K. H. Burrell, P. Monier-Garbet, B. W. Rice, D. P. Schissel, W. P. West, and R. D. Wood, Nucl. Fusion **38**, 387 (1998).
[30] R. V. Budny, Nucl. Fusion **34**, 1247 (1994).
[31] W. W. Heidbrink, P. L. Taylor, and J. A. Phillips, Rev. Sci. Instrum. **68**, 536 (1997).

[32]W. W. Heidbrink, J. Kim, and R. J. Groebner, Nucl. Fusion **28**, 1897 (1988).
[33]J. D. Strachan *et al.*, Nucl. Fusion **21**, 67 (1981).
[34]E. M. Carolipio and W. W. Heidbrink, Rev. Sci. Instrum. **68**, 304 (1997).
[35]W. W. Heidbrink, C. W. Barnes, G. W. Hammett *et al.*, Phys. Fluids B **3**, 3167 (1991).
[36]E. Ruskov, W. W. Heidbrink, and R. V. Budny, Nucl. Fusion **35**, 1099 (1995).
[37]D. L. Book, NRL Plasma Formulary, Naval Research Laboratory, Washington, D.C., 1990.
[38]P. Beiersdorfer, A. L. Roquemore, and R. Kaita, Rev. Sci. Instrum. **58**, 2092 (1987).